Strong Premelting Effect in the Elastic Properties of hcp-Fe Under Inner-Core Conditions

Benjamí Martorell *et al.*

Science **342**, 466 (2013);
DOI: 10.1126/science.1243651

acquire MI signatures from the ozone formation reaction (*9*) (Fig. 3C) via atomic oxygen interaction, creating small reservoirs with large positive $\Delta^{17}O$ and vice versa (e.g., atmospheric O_2 with negative $\Delta^{17}O$). Similarly, in meteorites, a large negative MI effect in minor phases (CAIs, chondrules and matrices in carbonaceous chondrites, and Ureilites) and a smaller positive MI effect in the more abundant classes (by mass, for example, ordinary chondrites and Rumaruti classes) are observed. Meteoritic negative and positive $\Delta^{17}O$ reservoirs could have been originated during the actual gas-to-particle formation process as experimentally demonstrated here (Fig. 3D). Solar system oxygen is more complicated, and the initial solar nebular bulk composition is inadequately defined. The measured oxygen composition of solar wind from Genesis concentrator is enriched in ^{16}O compared with CAIs (*30*), but the oxygen isotopic fractionation between the solar photosphere and the solar wind is not well established and presently an open question.

The final step in the formation of solid silicate from the gas-dominated nebula is a chemical reaction, and the fractionation occurring in this process should be considered regardless of which model is invoked. This reaction, if it occurs in a solar nebula at high temperature, the effect may be larger than observed in the present experiments given the inverse temperature dependency as observed for ozone (*31*). Last, the observed MI effect is unique to oxygen. The terminal atom regulates the formation and stabilization of vibrationally excited symmetrically structured molecules (*31*, *32*), and oxygen plays this critical role in SiO_2. This accounts for why other isotope systems (e.g., Si) do not correlate with oxygen and produce an observable symmetry-dependent fractionation. Carbon and hydrogen are candidates but only possess two stable isotopes and cannot prove the effect, and sulfur, with multiple valence states and exchangeability, is not ideal for preserving the effect.

References and Notes

1. R. N. Clayton, L. Grossman, T. K. Mayeda, *Science* **182**, 485–488 (1973).
2. J. N. Connelly *et al.*, *Science* **338**, 651–655 (2012).
3. R. N. Clayton, *Annu. Rev. Earth Planet. Sci.* **35**, 1–19 (2007).
4. M. H. Thiemens, *Annu. Rev. Earth Planet. Sci.* **34**, 217–262 (2006).
5. H. C. Urey, *J. Chem. Soc.* **1947**, 562–581 (1947).
6. M. F. Miller, *Geochim. Cosmochim. Acta* **66**, 1881–1889 (2002).
7. J. R. Lyons, E. D. Young, *Nature* **435**, 317–320 (2005).
8. J. Bally, W. D. Langer, *Astrophys. J.* **255**, 6 (1982).
9. M. H. Thiemens, J. E. Heidenreich 3rd, *Science* **219**, 1073–1075 (1983).
10. J. E. Heidenreich, M. H. Thiemens, *J. Chem. Phys.* **84**, 2129 (1986).
11. Y. Q. Gao, R. A. Marcus, *Science* **293**, 259–263 (2001).
12. R. A. Marcus, *J. Chem. Phys.* **121**, 8201–8211 (2004).
13. J. Savarino, M. H. Thiemens, *J. Phys. Chem. A* **103**, 9221–9229 (1999).
14. T. Röckmann *et al.*, *Science* **281**, 544–546 (1998).
15. A. K. Huff, M. H. Thiemens, *Geophys. Res. Lett.* **25**, 3509–3512 (1998).
16. E. Bouisset *et al.*, *J. Phys. At. Mol. Opt. Phys.* **24**, 1609–1614 (1991).
17. M. H. Thiemens, *Science* **283**, 341–345 (1999).
18. S. K. Bhattacharya, M. H. Thiemens, *Z. Natur. Teil A* **44**, 435 (1989).
19. A. Pandey, S. K. Bhattacharya, *J. Chem. Phys.* **124**, 234301 (2006).
20. M. Alagia, N. Balucani, P. Casavecchia, D. Stranges, G. G. Volpi, *J. Chem. Phys.* **98**, 8341 (1993).
21. J. Li *et al.*, *J. Chem. Phys.* **136**, 041103 (2012).
22. X. Song, J. Li, H. Hou, B. Wang, *J. Chem. Phys.* **125**, 6 (2006).
23. M. Brouard, D. W. Hughes, K. S. Kalogerakis, J. P. Simons, *J. Phys. Chem. A* **102**, 9559–9564 (1998).
24. M. H. Thiemens, S. Chakraborty, G. Dominguez, *Annu. Rev. Phys. Chem.* **63**, 155–177 (2012).
25. S.-H. Cho, J. Kim, *Astron. J.* **144**, 129 (2012).
26. V. Bujarrabal, J. Alcolea, P. Planesas, *Astron. Astrophys.* **257**, 14 (1992).
27. G. J. MacPherson, A. Boss, *Proc. Natl. Acad. Sci. U.S.A.* **108**, 19152–19158 (2011).
28. F. J. Ciesla, J. N. Cuzzi, *Icarus* **181**, 178–204 (2006).
29. C. Walsh, T. J. Millar, H. Nomura, *Astrophys. J.* **722**, 1607 (2010).
30. K. D. McKeegan *et al.*, *Science* **332**, 1528–1532 (2011).
31. Y. Q. Gao, R. A. Marcus, *J. Chem. Phys.* **116**, 137 (2002).
32. M. V. Ivanov, D. Babikov, *Proc. Natl. Acad. Sci. U.S.A.*, published online 19 February 2013 (10.1073/pnas.1215464110).

Acknowledgments: The authors thank the three anonymous reviewers for their helpful critical comments, which helped improve the manuscript. S.C. and M.H.T. acknowledge funding support from NASA Cosmochemistry (NNX09AG93G) and Origins in Solar System (NNX11AB39G) programs. We acknowledge G. Dominguez for helping to develop the kinetic model and helpful discussion with members of the Thiemens research group. Data described in this paper are presented in supplementary materials.

Supplementary Materials

www.sciencemag.org/content/342/6157/463/suppl/DC1
Materials and Methods
Supplementary Text
Figs. S1 to S4
Tables S1 to S5
References (*33*–*70*)

21 June 2013; accepted 11 September 2013
10.1126/science.1242237

Strong Premelting Effect in the Elastic Properties of hcp-Fe Under Inner-Core Conditions

Benjamí Martorell,* Lidunka Vočadlo, John Brodholt, Ian G. Wood

The observed shear-wave velocity V_S in Earth's core is much lower than expected from mineralogical models derived from both calculations and experiments. A number of explanations have been proposed, but none sufficiently explain the seismological observations. Using ab initio molecular dynamics simulations, we obtained the elastic properties of hexagonal close-packed iron (hcp-Fe) at 360 gigapascals up to its melting temperature T_m. We found that Fe shows a strong nonlinear shear weakening just before melting (when $T/T_m > 0.96$), with a corresponding reduction in V_S. Because temperatures range from $T/T_m = 1$ at the inner-outer core boundary to $T/T_m \approx 0.99$ at the center, this strong nonlinear effect on V_S should occur in the inner core, providing a compelling explanation for the low V_S observed.

Earth's inner core is predominantly made of iron (Fe), but it is commonly assumed to contain 5 to 10% Ni (*1*) and also light elements such as Si, C, and S, ~2 to 3 weight percent in total (*1*, *2*). Seismic wave velocities through the inner core are known, but at present, seismological and mineralogical models for the inner core do not agree (*3*–*9*). A major discrepancy between the observed seismic data and current mineralogical models derived from ab initio calculations is that these mineralogical models predict a shear-wave velocity V_S that is up to 30% greater than the seismically observed values (*4*, *9*, *10*). The addition of small quantities of Ni under these conditions does not reduce V_S by a sufficient amount to explain this (*9*), and although the effect of light elements on the velocities of Fe is not totally clear at inner-core conditions (*11*, *12*), all studies show that light-element effects are too small [<5% in V_S for 7% molar fraction in Si at 5000 K and 13,000 kg m^{-3} (*11*)] to solve the discrepancy.

Another possible cause of the discrepancy between mineralogical models and seismic data is that the elastic constants of Fe may soften drastically and nonlinearly very near to its melting point T_m, as has been observed in other metals. For instance, the shear modulus of Sn has been experimentally and theoretically shown to decrease by more than 50% at temperatures within ~1% of its melting point (*13*, *14*). According to ab initio simulations, the melting point of pure Fe at the conditions of the inner core is in the range 6200 to 6900 K (*15*–*17*) according to phase coexistence calculations (solid and liquid), with upper limit estimates up to 7500 K (*18*) when only the solid phase is heated until melting. The highest temperature for which the elastic properties of hcp-Fe have been obtained computationally is 6000 K (*5*); however, relative to the melting

Department of Earth Sciences, University College London, London WC1E 6BT, UK.

*Corresponding author. E-mail: b.massip@ucl.ac.uk

point of this simulation, T/T_m is probably ~0.8 and so this temperature is likely to be too low to reveal any strong elastic shear weakening just below melting.

To examine whether premelting effects in the elasticity of Fe can resolve the discrepancy in V_S between mineralogy and seismology, we simulated the effect of temperature on V_S at 360 GPa for hcp-Fe up to its melting point. We performed periodic ab initio calculations based on density functional theory (DFT) derived from quantum mechanics, coupled with molecular dynamics to obtain the elastic properties of hcp-Fe at finite temperatures (*19*).

Simulations of hcp-Fe at 360 GPa and at temperatures of 6600, 7000, 7250, and 7340 K (*19*), together with previous simulations at the same pressure and lower temperatures (*9*), indicated that the behavior of the elastic constants up to ~6600 K (Fig. 1) is very similar to that found in our earlier work on hcp-Fe at ~315 GPa and temperatures up to 5500 K (*20*). Specifically, elastic constants [defined as the ratio of applied stress on a material to the strain produced (*19*)] c_{11}, c_{33}, and c_{44} decreased with temperature, and c_{12} and c_{13} slightly increased (Fig. 1). However, one important difference between the simulations at 360 GPa and 315 GPa is that at higher pressure c_{33} is always larger than c_{11}; this finding suggests a large pressure dependence for the c_{11}-c_{33} crossover.

Above 6600 K, our calculations show that all of the elastic constants decreased with temperature, with some of them displaying very strong temperature dependence (Fig. 1). In particular, c_{44}, c_{12}, and c_{11} dropped by 46%, 19%, and 32%, respectively, from 7000 to 7340 K. This pronounced drop for a temperature increase of only 340 K indicates that the calculations above 7000 K are approaching the melting point of the simulated system. Analysis of the radial distribution functions and the root-mean-square displacements of the atoms, however, confirmed that the system remained completely solid during the simulation at 7340 K (fig. S1). A simulation at 8000 K melted completely after 16 ps (*19*).

The temperature dependence of the shear modulus (G) reveals an almost linear decrease up to 7000 K, followed by an abrupt drop beyond this point (fig. S2). Most models for G versus T describe only the linear region [e.g., the mechanical threshold stress model or the Steinberg-Cochran-Guinan model (*21*, *22*)] and do not describe its behavior close to the melting temperature. For this reason, Nadal and Le Poac [NP (*13*)] implemented a new model, based on Lindemann melting theory, that accounts for both the linear region and the region close to the melting temperature. Using this model (*19*), we obtained a Lindemann coefficient of $f = 0.112$ and a melting temperature of 7350 K for hcp-Fe at 360 GPa. The f coefficient is a material-dependent parameter and is normally between 0.1 and 0.3 (*23*); hence, our value falls in a reasonable range.

We note that the melting temperature obtained in this way is ~850 K higher than that expected from previous ab initio simulations (*16*, *17*), which used the phase coexistence method. This reflects the fact that the goal of the present work is not to obtain an accurate estimate for the melting temperature of hcp-Fe at 360 GPa, but rather to investigate the behavior of its elastic constants (and therefore the seismic velocities) very close to melting. To obtain the elastic constants, our simulations needed to be performed on a system with no preexisting surface or defects (such as the solid-liquid interface required for the phase coexistence approach), and it is well known that melting temperatures obtained in such a homogeneous system (mechanical melting) are substantially higher than the true thermodynamic (or heterogeneous) melting temperature (*24*, *25*). The melting temperature obtained here using the Nadal–Le Poac model is about 15% higher than that obtained using free energies or phase coexistence methods and is in accord with previous work showing that homogeneous melting temperatures are about 20% higher than the heterogeneous melting temperatures (*26*–*31*).

Although the strong decrease in elastic moduli in Fe observed here is seen close to the homogeneous melting temperature, there is good evidence that this also happens in a real heterogeneous sample. First, the experimentally measured elastic constants of Sn show a strong weakening at $T/T_m \approx 0.99$, where T_m is the true heterogeneous melting temperature. Second, this decrease has also been observed in atomistic simulations in body-centered cubic (bcc) vanadium at $T/T_m \approx 0.98$ (*24*). Third, the strong elastic weakening is associated with a rapid increase in defects (defined as over- or undercoordinated atoms), and this occurs at both the homogeneous and heterogeneous melting temperatures (*27*–*31*). The only difference in the heterogeneous case is that surface and preexisting defects can propagate into the bulk at a lower temperature than in a homogeneous solid. The number of atomic defects in our simulation jumped from 34% at 7340 K to 70% at 8000 K (*19*) (fig. S3). This is in very good agreement with previous simulations on much larger systems (*27*–*31*). Thus, it is relative temperature (T/T_m) rather than absolute temperature that is important.

Both compressional-wave (V_P) and V_S velocities decreased almost linearly with temperature up to ~7000 K at 360 GPa, with a substantial drop beyond this point (Fig. 2). The temperatures at which the velocities from the Preliminary Reference Earth Model (PREM) and our NP-like (like NP model but for velocities instead of G) model agree (7130 K for V_P and 7250 K for V_S) are at T/T_m values of 0.971 and 0.988, respectively, relative to the melting temperature of the simulation. Using an adiabatic geotherm (*32*), we find that the center of Earth should be ~200 K hotter than the inner-core boundary (ICB), whereas the melting line at the center of the inner core is 280 K above the temperature at the ICB (*17*); this leads to a value at the center of the inner core of $T/T_m = 0.988$. Thus, the core does indeed lie in a range of T/T_m where the velocities might be expected to be strongly decreased near melting.

Our results show that V_P and V_S for the inner core can be fitted with pure Fe for a physically sensible value of T/T_m. However, our simulated density of pure Fe is ~3% too high, and so the presence of light elements is still required to match inner-core values (table S1), but we would expect Fe with a few percent light elements to also show a strong shear softening near the melting temperature. If we assume that the light elements reduce the melting temperature of the Fe alloy, then the softening will occur at lower temperatures than in pure Fe, putting it in a more reasonable

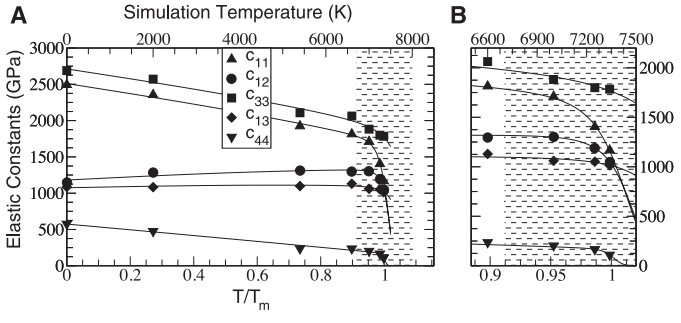

Fig. 1. Calculated elastic constants for hcp-Fe as a function of simulation temperature at 360 GPa. The solid black curves are fits to NP-like models (*19*). The gray band represents the minimum and maximum melting temperatures (*18*). The points below 6000 K are from (*9*). (**A**) The complete temperature range. (**B**) Results in the nonlinear regime.

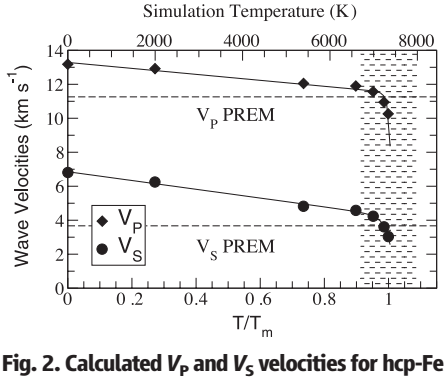

Fig. 2. Calculated V_P and V_S velocities for hcp-Fe as a function of T/T_m and simulation temperature at 360 GPa. The solid black curves are fits to NP-like models (*19*). The gray band represents the minimum and maximum melting temperatures for hcp-Fe (*18*). The points below 6000 K are from (*9*).

range of likely core temperatures. However, further investigations into multicomponent systems are essential to fully understand their effect on the elastic properties of the core. Overall, our results demonstrate that the inner core is likely to be in the strongly nonlinear regime; hence, there is no need to invoke special circumstances such as strong anelasticity, partial melts, or combinations of crystalline phases in order to match the observed seismic velocities and densities of the inner core.

References and Notes

1. F. Birch, *J. Geophys. Res.* **69**, 4377–4388 (1964).
2. J.-P. Poirier, *Phys. Earth Planet. Inter.* **85**, 319–337 (1994).
3. A. Cao, B. Romanowicz, N. Takeuchi, *Science* **308**, 1453–1455 (2005).
4. L. Vočadlo, *Earth Planet. Sci. Lett.* **254**, 227–232 (2007).
5. X. Sha, R. E. Cohen, *Phys. Rev. B* **81**, 094105–094110 (2010).
6. X. Sha, R. E. Cohen, *Geophys. Res. Lett.* **37**, L10302–L10305 (2010).
7. D. Antonangeli *et al.*, *Earth Planet. Sci. Lett.* **225**, 243–251 (2004).
8. A. P. Kantor *et al.*, *Phys. Earth Planet. Inter.* **164**, 83–89 (2007).
9. B. Martorell, J. Brodholt, I. G. Wood, L. Vočadlo, *Earth Planet. Sci. Lett.* **365**, 143–151 (2013).
10. A. M. Dziewonski, D. L. Anderson, *Phys. Earth Planet. Inter.* **25**, 297–356 (1981).
11. D. Antonangeli *et al.*, *Earth Planet. Sci. Lett.* **295**, 292–296 (2010).
12. Z. Mao *et al.*, *Proc. Natl. Acad. Sci. U.S.A.* **109**, 10239–10244 (2012).
13. M.-H. Nadal, P. Le Poac, *J. Appl. Phys.* **93**, 2472–2480 (2003).
14. M.-H. Nadal, C. Hubert, G. Ravel-Chapuis, *J. Alloys Compds.* **444–445**, 265–267 (2007).
15. D. Alfè, G. D. Price, M. J. Gillan, *Phys. Rev. B* **65**, 165118 (2002).
16. D. Alfè, *Phys. Rev. B* **79**, 060101–060104 (2009).
17. E. Sola, D. Alfè, *Phys. Rev. Lett.* **103**, 078501–078504 (2009).
18. G. Morard, J. Bouchet, D. Valencia, S. Mazevet, F. Guyot, *High Energy Density Phys.* **7**, 141–144 (2011).
19. See supplementary materials on *Science* Online.
20. L. Vočadlo, D. Dobson, I. G. Wood, *Earth Planet. Sci. Lett.* **288**, 534–538 (2009).
21. Y. P. Varshni, *Phys. Rev. B* **2**, 3952–3958 (1970).
22. M. W. Guinan, D. J. Steinberg, *J. Phys. Chem. Solids* **35**, 1501–1512 (1974).
23. D. R. Nelson, *Defects and Geometry in Condensed Matter Physics* (Cambridge Univ. Press, Cambridge, 2002).
24. V. Sorkin, E. Polturak, J. Adler, *Phys. Rev. B* **68**, 174102–174107 (2003).
25. V. Sorkin, E. Polturak, J. Adler, *Phys. Rev. B* **68**, 174103–174109 (2003).
26. K. Lu, Y. Li, *Phys. Rev. Lett.* **80**, 4474–4477 (1998).
27. F. Delogu, *J. Phys. Chem. B* **110**, 12645–12652 (2006).
28. F. Delogu, *J. Phys. Chem. B* **110**, 3281–3287 (2006).
29. F. Delogu, *J. Phys. Condens. Matter* **18**, 5639–5653 (2006).
30. G. Manai, F. Delogu, *Physica B* **392**, 288–297 (2007).
31. G. Manai, F. Delogu, *J. Mater. Sci.* **42**, 6672–6683 (2007).
32. J. P. Poirier, *Introduction to the Physics of the Earth's Interior* (Cambridge Univ. Press, Cambridge, 2000), pp. 230–244.

Acknowledgments: Supported by Natural Environment Research Council grant NE/H003975/1 (L.V.). Calculations were performed in the HECTOR supercomputer facility. Computer code VASP is available at www.vasp.at. The data presented in this paper are given in the main text and in the supplementary materials. B.M. performed research, analyzed data, and wrote the paper. L.V. designed research, analyzed data, and wrote the paper. J.B. analyzed data and wrote the paper. I.G.W. designed the research, analyzed data, and wrote the paper.

Supplementary Materials

www.sciencemag.org/content/342/6157/466/suppl/DC1
Materials and Methods
Supplementary Text
Figs. S1 to S3
Table S1
References (*33*–*43*)

23 July 2013; accepted 26 September 2013
Published online 10 October 2013;
10.1126/science.1243651

Atypical Combinations and Scientific Impact

Brian Uzzi,[1,2] Satyam Mukherjee,[1,2] Michael Stringer,[2,3] Ben Jones[1,4]*

Novelty is an essential feature of creative ideas, yet the building blocks of new ideas are often embodied in existing knowledge. From this perspective, balancing atypical knowledge with conventional knowledge may be critical to the link between innovativeness and impact. Our analysis of 17.9 million papers spanning all scientific fields suggests that science follows a nearly universal pattern: The highest-impact science is primarily grounded in exceptionally conventional combinations of prior work yet simultaneously features an intrusion of unusual combinations. Papers of this type were twice as likely to be highly cited works. Novel combinations of prior work are rare, yet teams are 37.7% more likely than solo authors to insert novel combinations into familiar knowledge domains.

Scientific enterprises are increasingly concerned that research within narrow boundaries is unlikely to be the source of the most fruitful ideas (*1*). Models of creativity emphasize that innovation is spurred through original combinations that spark new insights (*2*–*10*). Current interest in team science and how scientists search for ideas is premised in part on the idea that teams can span scientific specialties, effectively combining knowledge that prompts scientific breakthroughs (*11*–*15*).

Yet the production and consumption of boundary-spanning ideas can also raise well-known challenges (*16*–*21*). If, as Einstein believed (*21*), individual scientists inevitably become narrower in their expertise as the body of scientific knowledge expands, then reaching effectively across boundaries may be increasingly challenging (*4*), especially given the difficulty of searching unfamiliar domains (*17*, *18*). Moreover, novel ideas can be difficult to absorb (*19*) and communicate, leading scientists to intentionally display conventionality. In his *Principia*, Newton presented his laws of gravitation using accepted geometry rather than his newly developed calculus, despite the latter's importance in developing his insights (*22*). Similarly, Darwin devoted the first part of the *Origin of Species* to conventional, well-accepted knowledge about the selective breeding of dogs, cattle, and birds. From this viewpoint, the balance between extending science with atypical combinations of knowledge while maintaining the advantages of conventional domain-level thinking is critical to the link between innovativeness and impact. However, little is known about the composition of this balance or how scientists can achieve it.

In this study, we examined 17.9 million research articles in the Web of Science (WOS) to see how prior work is combined. We present facts that indicate (i) the extent to which scientific papers reference novel versus conventional combinations of prior work, (ii) the relative impact of papers based on the combinations they draw upon, and (iii) how (i) and (ii) are associated with collaboration.

We considered pairwise combinations of references in the bibliography of each paper (*23*, *24*). We counted the frequency of each co-citation pair across all papers published that year in the WOS and compared these observed frequencies to those expected by chance, using randomized citation networks. In the randomized citation networks, all citation links between all papers in the WOS were switched by means of a Monte Carlo algorithm. The switching algorithm preserves the total citation counts to and from each paper and the distribution of these citation counts forward and backward in time to ensure that a paper (or journal) with n citations in the observed network will have n citations in the randomized network. For both the observed and the randomized paper-to-paper citation networks, we aggregated counts of paper pairs into their respective journal pairs to focus on domain-level combinations (*24*–*26*). In the data, there were over 122 million potential journal pairs created by the 15,613 journals indexed in the WOS.

[1]Kellogg School of Management, Northwestern University, 2001 Sheridan Road, Evanston, IL 60208, USA. [2]Northwestern Institute on Complex Systems, Northwestern University, 600 Foster, Evanston, IL 60208, USA. [3]Datascope Analytics, 180 West Adams Street, Chicago, IL 60603, USA. [4]National Bureau of Economic Research, 1050 Massachusetts Avenue, Cambridge, MA 02138, USA.

*Corresponding author. E-mail: bjones@kellogg.northwestern.edu